Title

Solution-State Interactions of Bis(pentamethylcyclopentadienyl)- ytterbium, Cp*{sub 2}Yb, with Trialkyl Phosphines and R{sub 3}PX Complexes [X =0, NR', Chr"]

Authors

Schwartz, D.J.
Andersen, R.A.

Publication Date

1995-06-01

LBL-37483
UC-401
Preprint

Lawrence Berkeley Laboratory
UNIVERSITY OF CALIFORNIA

CHEMICAL SCIENCES DIVISION

Submitted to Journal of the American Chemical Society

Solution-State Interactions of Bis(pentamethylcyclopentadienyl)-ytterbium, Cp^*_2Yb, with Trialkyl Phosphines and R_3PX Complexes [X = 0, NR´, CHR´´]

D.J. Schwartz and R.A. Andersen

June 1995

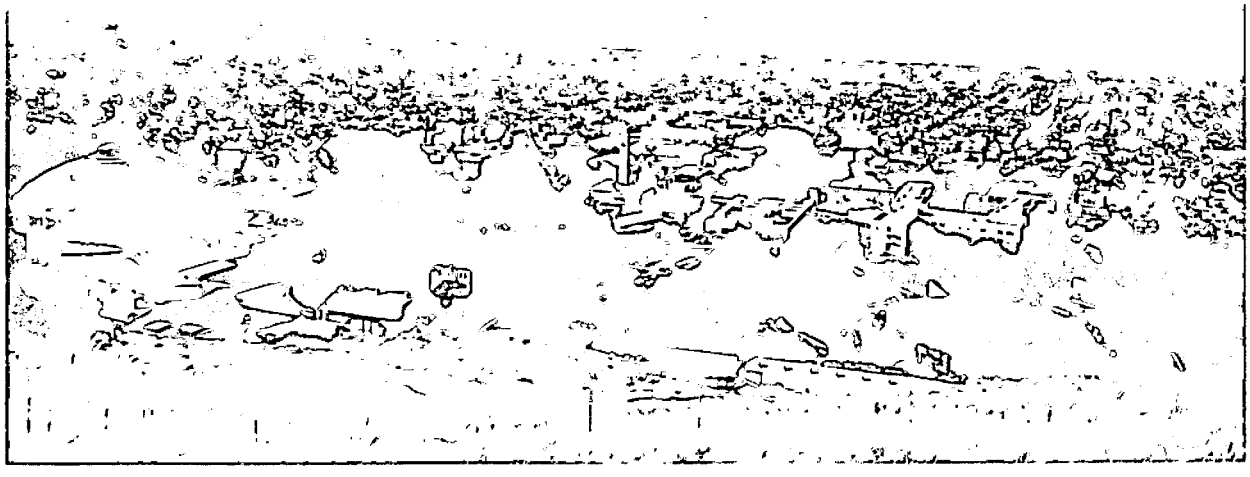

Prepared for the U.S. Department of Energy under Contract Number DE-AC03-76SF00098

DISCLAIMER

LBL-37483
UC-401

Solution-State Interactions of Bis(pentamethylcyclopentadienyl)-ytterbium, Cp^*_2Yb, with Trialkyl Phosphines and R_3PX Complexes [X = 0, NR´, CHR´´]

David J. Schwartz and Richard A. Andersen

Department of Chemistry
University of California, Berkeley

and

Chemical Sciences Division
Lawrence Berkeley Laboratory
University of California
Berkeley, California 94720

June 1995

This work was supported by the Director, Office of Energy Research, Office of Basic Energy Sciences, Chemical Sciences Division, of the U.S. Department of Energy under Contract No. DE-AC03-76SF00098.

Abstract.

The interactions formed between Cp^*_2Yb (**1**) and phosphines and R_3PX derivatives (X = O, NR', CHR") in solution have been investigated using multinuclear (^1H, ^{13}C, ^{31}P, ^{171}Yb) and variable temperature NMR spectroscopy. Intermolecular exchange can be slowed at low temperature for 1:1 and 1:2 phosphine adducts, with a $^1J_{YbP}$ value of *ca.* 950 Hz for $Cp^*_2Yb(PEt_3)$ (**3**) and $Cp^*_2Yb(PMe_3)$ (**4**), and *ca.* 600 Hz for $Cp^*_2Yb(PMe_3)_2$ (**2**), Cp^*_2Yb(dmpm) (dmpm = $Me_2PCH_2PMe_2$) (**5**), and $Cp^*_2Yb(1,2\text{-}(PMe_2)_2C_6H_4)$ (**6**). Adducts of **1** with Me_3PO and Et_3PNH undergo slow intermolecular exchange in solution at 25 °C (NMR timescale); both 1:1 adducts ($Cp^*_2Yb(OPMe_3)$, **7**; $Cp^*_2Yb(HNPEt_3)$, **9**) and 1:2 adducts ($Cp^*_2Yb(OPMe_3)_2$, **8**; $Cp^*_2Yb(HNPEt_3)_2$, **10**) have been isolated. The spectroscopic properties of two ylide adducts, $Cp^*_2Yb(Me_2PhPCHSiMe_3)$ (**12**) and $Cp^*_2Yb(Me_2PhPCH_2)$ (**13**), have also been investigated. Intermolecular exchange can be slowed at low temperature in both cases; in the former complex a second process, resulting in inequivalent Cp^* rings and inequivalent P-bound methyl groups, can also be slowed at lower temperatures. The nature of this process is discussed in detail. The solid state structure of **12** has been determined, the crystal data are: monoclinic, space group Cc, with a = 14.776(8) Å, b = 14.852(8) Å, c = 15.186(9) Å, b = 104.80(4)°, V = 3222(3) $Å^3$, Z = 4, final R = 0.0500 for 154 variables and 1874 data with $(F_o)^2 > 3\sigma(F_o)^2$. The NMR values for all of the complexes are discussed in detail. In addition, the ^{171}Yb chemical shifts for **6**, **7**, and **12** have been measured, *via* $^1H/^{171}Yb$ indirect detection utilizing long-range J_{YbH} coupling, and are discussed.

Introduction

Weak interactions in solution between organometallic complexes and organic substrates have been implicated in a variety of important reactions, including C-H bond activation[1] and the Ziegler-Natta polymerization of olefins.[2] Consequently, a thorough understanding of the electronic and geometric consequences of such interactions is desirable.

The lanthanide metallocene Cp^*_2Yb (**1**) possesses several properties that make it amenable to the investigation of weak metal-ligand interactions in solution: it is bent,[3] thus requiring little reorganization energy upon binding of a third ligand; it is diamagnetic ($4f^{14}$ electronic configuration) and possesses an NMR-active metal isotope (^{171}Yb: I = 1/2, 14.3%), allowing the use of NMR spectroscopy as an investigative tool; and the Yb center is Lewis-acidic. Several adducts of **1** (or related derivatives) with non-classical Lewis bases have been isolated and characterized in the solid state; several of these adducts are shown in Figure 1.[4,5]

(Figure 1 here)

All of the previously-reported $Cp^*_2YbL_n$ adducts were found to undergo fast intermolecular exchange in solution at all temperatures, on the NMR timescale, precluding a detailed study of the solution-state perturbations that result from the weak interactions present.

Given the favorable properties of **1** for such investigations, and the relative paucity of such studies (especially for the lanthanides and actinides, a result of the paramagnetism of almost all Ln/An complexes[6]), we felt such a study would be worthwhile, and have recently undertaken an investigation of slow-exchange $Cp^*_2YbL_n$ systems. We have recently reported the details of the solution-state interactions formed between **1** and *cis*-

P_2PtX_2 complexes (X = H, Me);[7] these adducts undergo slow intermolecular exchange in solution, and spin-spin coupling between the ^{171}Yb isotope and the ^{1}H, ^{13}C, ^{31}P, and ^{195}Pt nuclei of the P_2PtX_2 ligands is resolved.

Phosphine complexes of the lanthanides and actinides are relatively rare,[8] as a result of the hard nature of these metal centers and the soft nature of phosphines. Almost no solution-state investigations have been reported for lanthanide and actinide complexes in general, and for phosphine derivative complexes, more specifically. Herein, we report the results of an investigation of the solution-state interactions formed between **1** and phosphines, phosphine oxides (R_3PO), phosphine imines (R_3PNR'), and phosphine ylides (R_3PCHR''). The strength and nature of the interactions formed between **1** and phosphines, phosphine oxides and imines, and the isoelectronic (to phosphine oxides and imines) ylides, have been found to vary significantly. In addition, a novel intramolecular dynamic process of an ylide adduct of **1** has been elucidated.

Results

Interactions with Phosphines. Addition of 2 eq. of PMe_3 to a dark brown toluene solution of **1** gives a bright green solution, from which green crystals of $Cp^*_2Yb(PMe_3)_2$ (**2**) may be isolated in 88% yield upon cooling to -80 °C. A similar synthetic procedure with 2 eq. of PEt_3 yields dark blue crystals of the 1:1 adduct $Cp^*_2Yb(PEt_3)$ (**3**), presumably a result of the larger size of PEt_3 relative to PMe_3. The ^{1}H and $^{31}P\{^{1}H\}$ NMR spectral values of **2** and **3** at 25 °C are very similar to the spectral values for the free compounds, showing that the solution-state interaction between **1** and these phosphines is relatively weak. The phosphine alkyl group protons and the phosphorus nucleus are not coupled to the ^{171}Yb nucleus, indicating fast intermolecular exchange occurs on the NMR timescale for both **2** and **3**.

Cooling a toluene-d_8 sample of the 1:2 PMe_3 adduct **2** to -101 °C results in broadened resonances in both the ^{1}H and $^{31}P\{^{1}H\}$ spectra (the values are given in Table 1), suggesting that the intermediate exchange region has been reached. Even though the

width at half height of the $^{31}P\{^{1}H\}$ resonance (at -49.2 ppm) is 135 Hz, a $^{1}J_{YbP}$ value of *ca.* 600 Hz is resolved.

(Table 1 here)

The $^{31}P\{^{1}H\}$ spectrum of a sample of **1** with *ca.* 0.8 eq of PMe_3, at -83 °C, contains a sharp singlet at -45.4 ppm with ^{171}Yb satellites (Fig. 2, the area of each satellite is approximately 7% of the area of the major resonance, as expected), presumably arising from the 1:1 adduct $Cp^*_2Yb(PMe_3)$ (**4**).

(Figure 2 here)

The ^{171}Yb-^{31}P coupling is 956 Hz, roughly 2/3 larger than the analogous value for the 1:2 PMe_3 adduct **2**. The ^{1}H spectrum of this sample at -83 °C contains resonances for both free and bound **1** (the spectral values are given in Table 1); coupling of ^{171}Yb to the alkyl protons of the bound phosphine ($^{3}J_{YbH}$) is not resolved. The slow exchange behavior of this sample at -83 °C, compared to the intermediate exchange observed for **2** at -101 °C, indicates that the barrier for intermolecular exchange is higher for **4** than for **2**; this will be discussed below.

Cooling a toluene-d_8 sample of the 1:1 PEt_3 adduct, **3**, to -103 °C results in slow intermolecular exchange on the NMR timescale; the observed $^{1}J_{YbP}$ value of 950 Hz is similar to the analogous value observed for the 1:1 PMe_3 derivative, **4**. Again, $^{3,4}J_{YbH}$ is not resolved (the NMR values for this sample are also given in Table 1). The coalescence temperature of the free and bound Cp^* resonances is -89 °C.[9] The ^{1}H and $^{31}P\{^{1}H\}$ spectra of a sample of **1** and 2 eq. of PEt_3 contain broad resonances at -103 °C (^{31}P resonance, $w_{1/2}$ *ca.* 900 Hz), indicating that the exchange barrier is lower for the 2:1 PEt_3 derivative, relative to the 1:1 adduct, similar to the situation observed for the PMe_3 derivatives, above.

At this point, it was of interest to investigate the behavior of chelating phosphines with **1**. While $Cp^*_2Yb(dmpm)$ (**5**) has been reported,[8b] only the exchange-averaged room temperature NMR data were measured. Cooling a sample of **5** to -65 °C results in slow exchange, with a $^1J_{YbP}$ coupling of 580 Hz (values given in Table 1); this value is unchanged at -90 °C. As found for the monodentate phosphine analogues above, coupling of ^{171}Yb to the phosphine alkyl protons is not resolved. A sample of **5** containing a slight excess of dmpm exhibits intermediate exchange behavior at -65 °C; although two resonances are visible in the $^{31}P\{^1H\}$ spectrum, arising from free dmpm and **5**, both are broad, with widths at half height of *ca.* 450 Hz. This contrasts with the slow exchange behavior at this temperature for **5**, in the absence of added dmpm. A similar phenomenon, with a faster exchange rate in the presence of excess phosphine, was found for many of the phosphine adducts, and is likely a result of associative exchange in the presence of excess phosphine.[7,10]

The dmpe complex, $Cp^*_2Yb(dmpe)$, is insoluble in toluene and diethyl ether, but dissolves in thf to give $Cp^*_2Yb(thf)_2$ and the free phosphine.[8b] This behavior indicates that $Cp^*_2Yb(dmpe)$ likely has a polymeric structure, with dmpe acting as a bridging rather than a chelating ligand. Addition of $Me_2PCH_2P(Me)CH_2PMe_2$ to a toluene solution of **1** results in the instantaneous precipitation of a bright green solid, presumably also with a polymeric structure; the ^1H NMR spectrum of this solid dissolved in thf-d_8 indicates the presence of $Cp^*_2Yb(thf)_2$ and the free phosphine, in a 1:1 ratio. A toluene solution of **1** and 1,2-$(PMe_2)_2C_6H_4$, in a *ca.* 2:1 molar ratio, is dark green-brown. The ^1H spectrum of this sample at 25 °C contains a broad Cp^* resonance ($w_{1/2}$ = 35 Hz at 400 MHz), indicating intermediate intermolecular exchange; however, $^1J_{YbP}$ of 656 Hz is resolved in the $^{31}P\{^1H\}$ spectrum at this temperature (a result of the larger $^1J_{YbP}$ value, relative to the frequency difference between the free and bound Cp* resonances[11]). Cooling this sample results in decoalescence of the Cp* resonance into free and bound resonances, the latter arising from the 1:1 adduct $Cp^*_2Yb(1,2\text{-}(PMe_2)_2C_6H_4)$ (**6**); the $^1J_{YbP}$ value is unchanged

upon cooling. We believe that the *cis* disposition of the Me_2P groups in 1,2-$(PMe_2)_2C_6H_4$, in contrast to dmpe and $Me_2PCH_2P(Me)CH_2PMe_2$, enforces bidentate rather than bridging interactions.[12] The ^1H and $^{31}P\{^1H\}$ NMR values measured on **6** at -20 °C are given in Table 1. Coupling of the ^{171}Yb nucleus to the methyl protons of the phosphine ligand, $^3J_{YbPC\underline{H}3}$, is resolved and is 2.7 Hz (measured at -30 °C).[13] Using this coupling constant, the HMQC pulse sequence[14] was utilized to acquire a $^1H/^{171}Yb$ spectrum, at -30 °C (Figure 3). The ^{171}Yb (vertical) dimension of this spectrum shows that the ^{171}Yb chemical shift of **6** is +782 ppm (this value will be discussed below); ^{171}Yb-^{31}P coupling is resolved, and is identical to the value measured from the 1-D $^{31}P\{^1H\}$ spectrum.

(Figure 3 here)

From Table 1 it can be seen that a low field shift of the Cp^* resonance of **1**, of *ca.* 0.20 ppm, occurs upon binding of a phosphine ligand. Such low field shifts of the Cp^* resonance are common upon coordination of a ligand to **1**.[7] The ^1H chemical shifts of the phosphine alkyl groups move slightly upfield upon coordination to **1**; the shift for the 1:1 adduct **4** ($\Delta(\delta)$ = -0.24 ppm) is roughly twice the shift for the 1:2 adduct, **2** ($\Delta(\delta)$ = -0.14 ppm). While the $-CH_2$ resonance of PEt_3 is shifted upfield by only 0.03 ppm upon coordination to **1**, the methyl resonance is shifted upfield by a surprisingly large 0.51 ppm. This shift may be indicative of a γ-agostic interaction; agostic interactions have been observed in the solid state for adducts of **1**.[4b,7,15] However, the $^1J_{CH3}$ value of **3** at -103 °C is 127(1) Hz, unchanged from the analogous value for free PEt_3 at this temperature.[16]

The ^{31}P resonances for all of the phosphine complexes discussed above are shifted downfield *ca.* 13-21 ppm, consistent with the phosphines acting as Lewis bases towards the Yb center of **1**. The $^1J_{YbP}$ values for the 1:1 adducts **3** and **4** (956 Hz and 950 Hz, respectively) are roughly 60% larger than the analogous values for the 1:2 PMe_3 adduct **2**

and the dmpm and 1,2-$(PMe_2)C_6H_4$ adducts, **5** and **6**, respectively. This indicates that each Yb-P interaction in the 1:2 adducts (considering **5** and **6** as 1:2 adducts, as they each have two P donors/Yb center) is weaker than the single Yb-P interaction in the 1:1 adducts.[17] The similar spectral values for the 1:2 PMe_3 and dmpm adducts, **2** and **5** (δ (^{31}P) perturbations, $^1J_{YbP}$ values), indicate that chelation does not have a significant effect on the interactions formed between **1** and phosphines.[18]

Interactions with R_3PX Complexes (X = O, NR'). The $Cp^*_2Yb(OPMe_3)$ adduct (**7**), isolated in 83% yield as a yellow-orange crystalline solid, undergoes slow intermolecular exchange in C_6D_6 at 25 °C. This contrasts with the fast exchange behavior at 25 °C that was observed for the phosphine adducts discussed above. While ^{171}Yb-^{31}P coupling is observed for **7** ($^2J_{YbP}$ = 94.6 Hz), long-range ^{171}Yb-^1H coupling ($^4J_{YbH}$) is not resolved. The ^1H and ^{31}P spectral values for **7** and Me_3PO are given in Table 2. When a toluene-d_8 sample of **7** (with 1 eq. of excess **1**[10]) is heated in the NMR probe, coalescence of the free and bound Cp* resonances occurs at 110 °C.[9] The $^{31}P\{^1H\}$ spectrum of a sample of $Cp^*_2Yb(SPPh_3)$ in C_6D_6 shows $^2J_{YbP}$ of 87 Hz,[19] similar to the analogous value found for **7**.

(Table 2 here)

Addition of 2 eq. of Me_3PO to a toluene solution of **1** results in the precipitation of an orange solid, $Cp^*_2Yb(OPMe_3)_2$ (**8**), which is insoluble in toluene and aliphatic hydrocarbon solvents. The 1:2 adduct **8** dissolves in thf-d_8 with a slight darkening in color; the ^1H and $^{31}P\{^1H\}$ spectral features (broadened resonances, and slightly shifted Me_3PO chemical shift values, relative to those of free Me_3PO in thf-d_8) indicate competitive exchange with the solvent. While thf is competitive with Me_3PO as a ligand towards the Yb center of **1**, when thf is removed under reduced pressure, the pure complex **8** is re-isolated. When Et_2O is added to a sample of the 1:1 adduct **7**, a green solution with an

orange precipitate results. Apparently, Et_2O can coordinate to an empty coordination site on the Yb center, lowering the barrier to intermolecular exchange (similar to the phenomenon discussed above for samples of **1** containing excess phosphine). The result is precipitation of the orange 1:2 adduct **8** and a solution containing the green $Cp^*_2Yb(Et_2O)$ adduct, the identity of which was confirmed by ^1H NMR spectroscopy.[21]

The interaction formed between **1** and the phosphine imine Et_3PNH is similar to that found for Me_3PO. The ^1H NMR spectrum at 25 °C of a toluene-d_8 sample of the light orange $Cp^*_2Yb(HNPEt_3)$ adduct (**9**) indicates slow intermolecular exchange; a $^2J_{YbP}$ value of 91.6 Hz can be measured from the $^{31}P\{^1H\}$ spectrum. The values for this sample, and for uncomplexed Et_3PNH, are given in Table 2. Unfortunately, the ^1H resonance for the N-H proton is not resolved in either of these samples, at 25 °C or at -90 °C, presumably a result of ^{14}N quadrupolar or exchange broadening.[22] When 2 eq. of Et_3PNH are added to a toluene solution of **1**, the orange 1:2 adduct $Cp^*_2Yb(HNPEt_3)_2$ (**10**) precipitates from solution. Similar to **8**, this solid dissolves in thf-d_8, giving ^1H and $^{31}P\{^1H\}$ spectra that indicate competitive exchange with the solvent. A sample of **1** (2 eq.) and $Et_3PN(SiMe_3)$[23] undergoes fast exchange at 25 °C, on the NMR timescale. However the ^1H spectrum of this sample at -83 °C contains resonances for both free and bound Cp* rings (T_c = -50 °C[9]), and ^{171}Yb-^{31}P coupling is resolved in the $^{31}P\{^1H\}$ spectrum ($^2J_{YbP}$ = 7(1) Hz, values given in Table 2). The fast intermolecular exchange at 25 °C for $Cp^*_2Yb(Et_3PNSiMe_3)$ (**11**), as well as the much smaller $^2J_{YbP}$ value as compared to **9** ($^2J_{YbP}$ = 91.6 Hz), likely result from the sterically bulky $SiMe_3$ group preventing the Yb center from approaching the nitrogen nucleus as closely as in the Et_3PNH derivative, **9**.

Interactions with R_3PCHR' Complexes. Considering the relatively strong interactions formed between **1** and phosphine oxides and imines, it was of interest to examine the interaction of **1** with isoelectronic phosphine ylides. Two resonance forms can be drawn for phosphine ylides (Fig. 4), and the chemical properties of ylides show that both forms are important.

(Figure 4 here)

It is known that ylides generally have a slightly pyramidal geometry about the ylide carbon atom in the solid state,[24,25] $^1J_{CH}$ coupling constants suggesting sp^2 hybridization,[26,27] P-C distances consistent with a P=C double bond,[25,26] a low barrier to rotation about the P-C bond,[24,28] and bind strongly to alkali metals *via* the carbon center.[26] Ylides typically also interact with transition metals*via* the carbon center.[24,29] Recent *ab initio* molecular orbital calculations have found that the dominant resonance structure for phosphine ylides is the ionic one.[24]

Addition of 1 eq. of $Me_2PhPCHSiMe_3$[30] to a toluene solution of **1** results in a dark green solution from which dark green crystals of $Cp^*_2Yb(Me_2PhPCHSiMe_3)$ (**12**) can be isolated in 55% yield. The ^1H and $^{31}P\{^1H\}$ spectra of a toluene-d_8 sample of **12**, containing an additional equivalent of **1**,[10] indicate that fast intermolecular exchange occurs at 25 °C. On cooling, two different fluxional processes can be distinguished, as indicated by the variable temperature ^1H spectra, from -3 °C to -98 °C (Fig. 5).

(Figure 5 here)

The slower process is intermolecular exchange of free and bound **1**; the averaged Cp^* resonance decoalesces into free and bound resonances upon cooling, with a T_c = -40 °C.[9] Further cooling results in inequivalent Cp^* rings, as well as inequivalent phosphorus-bound methyl groups. The coalescence temperatures (two slightly different temperatures for this one process, as a result of the frequency differences between the inequivalent Cp^* rings and the inequivalent methyl groups[11]) gives an approximate $\Delta G^{\ddagger}$ value of 9.2(2) kcal mol^{-1} for this fluxional process. The nature of these fluxional processes will be discussed in detail below.

A toluene-d_8 sample of the Me_2PhPCH_2[30] adduct, $Cp^*_2Yb(Me_2PhPCH_2)$ (**13**), with an additional equivalent of **1**, also undergoes fast intermolecular exchange at 25 °C; this exchange is slowed upon cooling ($T_c(Cp^*)$ = -68 °C[9]). The two identical groups on the ylide carbon necessarily result in equivalent Cp^* and PMe_2 groups at all temperatures. To investigate the details of the interactions between **1** and the ylides in solution, the ^1H, $^{13}C\{^1H\}$ and $^{31}P\{^1H\}$ NMR spectra were measured on samples of **12** and **13** (both samples containing 1 eq. excess of **1**), at -78 °C and -93 °C, respectively.[31] The spectral values of the two samples, as well as those of the two ylides at the same temperatures, are given in Table 3.

(Table 3 here)

Examination of the values in Table 3 shows the usual downfield shift of the Cp^* rings of **1**, and of the ^{31}P chemical shifts (the $\Delta(\delta P)$ values are slightly less than were observed for the phosphine, oxide, and imine derivatives, above), upon adduct formation.[32] Interestingly, the ylide proton resonance of **12** is shifted 0.69 ppm downfield from the value for the free ylide, while the analogous resonance for **13** is shifted in the opposite direction, by 0.65 ppm. The methyl and $SiMe_3$ spectral values are perturbed only slightly, consistent with a direct Yb-C interaction. The $^2J_{YbP}$ value for **12** is significantly smaller than the analogous value for **13**. This may be either a steric or an electronic effect; the sterically bulky $SiMe_3$ group is known to stabilize (i.e., delocalize) the ylidic negative charge.[26] The ^{13}C chemical shifts of the ylide carbons of both **12** and **13** are shifted downfield slightly upon adduct formation, consistent with C→Yb electron donation. The $^1J_{PC}$ values involving this carbon are roughly halved upon formation of the adducts; the values for **12** and **13** are similar to the analogous values for phosphonium salts, $(R_3PCHR'R'')^+$,[24] and for previously-reported M-ylide complexes.[33] Unfortunately, coupling between ^{171}Yb and the ylide ^1H and ^{13}C nuclei was not resolved, most likely a

result of line broadening from the low temperature required to slow intermolecular exchange.[34]

To investigate the details of the Yb-ylide interaction in the solid state, **12** was characterized by X-ray crystallography and an ORTEP diagram is shown in Fig. 6. There are relatively few structurally characterized lanthanide-ylide complexes.[36]

(Figure 6 here)

The crystallographic data, positional parameters, and selected intramolecular distances and angles are given in Tables 4-6. The quality of the X-ray data was not sufficient to locate the ylide-H; it is assumed to be oriented roughly downwards in Fig. 6, based on the positions of the Yb, Si, and P atoms. The quality of the data was also not sufficient to allow anisotropic refinement on the carbon atoms, see the Experimental section for details of the structure solution.

(Tables 4-6 here)

The Cp^*-Yb-Cp^* angle, the Yb-Cp^* distances, and the Cp^*-Yb-Cp^*/Si-C24-P torsional angle (84°) of **12** are within the expected ranges.[4,7] The Yb-C21 distance, 2.69(2) Å, is indicative of a direct Yb-C interaction.[4,5,35] The P-C21 distance of 1.69(2) Å is within the range observed for M-ylide complexes.[26,38] The Yb-C21-Si angle (105°) is more acute than the Yb-C21-P angle (128°), resulting in a short Yb-methyl contact involving one of the methyl carbons on the Si atom (Yb-C22 = 3.15(2) Å). This likely results from a secondary Yb-methyl interaction, as the sum of the Van der Waals radii[39] for a methyl group (2.00 Å) and Yb(II) is 3.70 Å.[15,40] Consistent with this, the C(ylide)-Si-C(methyl) angle involving this methyl carbon center is slightly smaller than the other two C-Si-C angles (C21-Si-C22, 106°; C21-Si-C23, 116°; C21-Si-C24, 112°). As the

hydrogen atoms were not located in the structure of **12**, further discussion on this point is not warranted. The Yb-C21-P angle, 128°, is within the expected range for M-ylide structures.[33b,41] Thus, interaction of **1** with $Me_2PhPCHSiMe_3$ involves a direct Yb-C interaction, supplemented by a secondary γ–CH_3 interaction, and adduct formation does not result in any unexpected perturbations of the ylide structure. The solid-state structure of **12**, with C_1 symmetry, is consistent with the low temperature NMR data for this complex.

Discussion

Assuming that the kinetic barrier to intermolecular exchange serves as a qualitative indication of the thermodynamic strength of the Yb-L interaction,[9,10,42] the ligands studied above can be roughly ordered in decreasing strength of interaction towards **1**. For the 1:1 adducts, Me_3PO, Et_3PNH > ylides, PMe_3, PEt_3. This is easily rationalized by noting that the best ligands have hard heteroatom donors with lone pairs. Ylides and monodentate phosphines are roughly similar with respect to binding strength to **1**. For the 1:2 adducts (including the bidentate phosphine derivatives in this class), dmpm and 1,2-$(PMe_2)_2C_6H_4$ form stronger interactions with **1** than $(PMe_3)_2$ and $(PEt_3)_2$, the chelate effect resulting in a slightly better interaction relative to the monodentate analogues.[18] The 1:2 monodentate phosphine adducts have a lower kinetic barrier to intermolecular exchange than the analogous 1:1 adducts, indicating a weaker interaction in the former adducts; this result is consistent with the smaller ^{171}Yb-^{31}P coupling constants for the 1:2 adducts (Table 1).[17]

Comparison of the J_{YbP} values found for the complexes studied in this work to J_{MP} values that have been reported in the literature is informative. There have been four $^1J_{YbP}$ values reported,[43] the most applicable being the values for $(Me_2\overline{PC(SiMe_3)PMe_2)_2}Yb(LiI)_2(thf)_3$ (497 Hz),[43b] and $Yb\overline{[N(SiMe_2CH_2PR_2)_2]_2}$ (R = Me, 665 Hz; R = Ph, 522 Hz);[43c] the ligands in these complexes all bear a negative charge, in contrast to the neutral phosphine ligands used in the present study. The reported values are similar to the $^1J_{YbP}$ values found for the 1:2 phosphine adducts in this study. There

have been several $^2J_{MP}$ values reported for transition metal-ylide complexes. The values reported (reduced coupling constants, K, in parentheses),[44] *cis*-$(Me_3PCH_2)_2PtMe_2$, 92 Hz (8.77);[45] $[(Me_3PCH_2)Rh(PMe_3)_2(Cp)]I_2$, 4.5 Hz (-2.92);[46] *trans*-$[Pt(CH_2PR_3)(PR_3)_2X][Y]$ (X, Y = halides), *ca.* 100 Hz (9.53);[41b] and *cis*-$[Pt(CH_2PR_3)(PR_3)_2X][Y]$ (X, Y = halides), *ca.* 50 Hz (4.76);[41b] are similar to the values found for **12** ($^2J_{YbP}$ = 8 Hz, K = 0.933) and **13** ($^2J_{YbP}$ = 37 Hz, K = 4.32). In addition, the slight increase in the ylide $^2J_{PCH}$ value upon formation of the interaction with **1**, as observed in **12** and **13**, is a common result of coordination of ylides to metal centers.[33]

Two different fluxional processes can be slowed upon cooling a sample of **12** from 25 °C to -98 °C. The first process involves intermolecular exchange of free and bound **1**, and slowing of the second process results in inequivalent PMe_2 groups and inequivalent Cp^* rings. As the Yb center is bound *via* the ylide carbon center, this carbon becomes chiral once intermolecular exchange is stopped, resulting in diastereotopic methyl groups. However, the methyl groups do not become inequivalent until a much lower temperature, at which point the Cp^* rings also become inequivalent (Fig. 5). Fast inversion of the chirality at the ylide carbon would make the PMe_2 groups equivalent. This fluxional process has an identical barrier as the process that results in equivalency of the bound Cp^* rings of **12** between -40 °C and -84 °C, and is most likely the same physical process.

Certain metal-ylide complexes are known to undergo phosphine exchange *via* metal carbene intermediates.[24,26] Addition of PMe_3 to a C_6D_6 solution of **12** results in no phosphine exchange after several hours at 25 °C, ruling out such a process. Consequently, the only way for fast inversion to occur at the ylide carbon is *via* fast interchange of **1** between the two ylide enantiofaces (Figure 7; the term enantioface is used with the P=C planar resonance form in mind).

(Figure 7 here)

Since intermolecular exchange is slow below -40 °C, this process must occur without exchange of free and bound molecules of **1**. It is reasonable to assume that inversion at the ylide carbon involves the Yb center, as this is the only "labile" ligand.

One possible mechanism for this inversion involves movement of **1** to the opposite ylide enantioface (the planar ylide resonance form is used for this discussion, for purposes of clarity)*via* a σ-complex involving the ylide C-H bond in the transition state (Fig. 8).[47]

(Figure 8 here)

This process, if fast on the NMR timescale, results in identical averaged environments for the two PMe_2 groups and for the two Cp^* rings. A similar process with enantioface migration *via* a σ-complex, involving an olefinic C-H bond, has recently been invoked by Peng and Gladysz to explain the observation of intramolecular equilibration of the diastereomeric chiral Re complex $[CpRe(NO)PPh_3)(H_2C{=}CHR)][BF_4]$.[48,49] As Peng and Gladysz have noted, σ-complex interactions have been estimated at *ca.* 10 kcal mol^{-1} and consequently, can stabilize the transition state with respect to dissociation (i.e., intermolecular exchange).[48] Interaction of the electron-rich C-H bond of the ylide with the electrophilic Yb center is likely a favorable interaction.

Another possible mechanism for this fluxional process involves complete cleavage of the Yb-ylide interaction, with retention of Yb-P spin-spin coupling; this possibility assumes the presence of a solvent-caged species, for explaining the lack of intermolecular exchange.[50] Considering the Yb-methyl interaction that is present in the (ground-state) solid state structure of **12** (Fig. 6, and accompanying discussion), it is also possible that the inversion at the ylide carbon center occurs *via* a Yb-methyl interaction; this possibility is very similar to the σ-complex mechanism discussed above. Given the experimental evidence, none of these three possible mechanisms can be rigorously ruled out.

The $^1J_{CH}$ value of the ylide C-H bond of **12** decreases by 25 Hz upon formation of the interaction with **1**, consistent with a direct Yb-C interaction. Protonation of Me_3PCH_2 results in a decrease in $^1J_{CH}$ from 149 Hz to 133 Hz,[51] while $^1J_{CH}$ for $Me_3PCH_2(Ni(CO)_3)$ (in which the Ni interacts with the ylide carbon, based on the solid-state structure of a related complex)[27] is 123 Hz. If there were a C-H-Yb interaction present in the ground state structure of **12**, the $^1J_{CH}$ value would probably be significantly smaller than the observed value of 111 Hz. Analogous $^1J_{CH}$ values for transition metal agostic complexes are reduced by as much as 50%, relative to the "free" values.[52] While it is clear that the ground state Yb-ylide interaction involves a direct Yb-C interaction (supplemented by a Yb-methyl interaction), this does not rule out the presence of a σ-complex in the transition state of the fluxional process, as discussed above.

Examination of Figure 3 shows that, in addition to the ^{171}Yb correlations from the PMe_2 protons, correlations to the bound Cp^* methyl protons are also present. This shows that spin-spin coupling between ^{171}Yb and these protons is present in **6**. We have measured the analogous value for **1**, and it is 2.5 Hz; this coupling will not vary much with the ligand, L, in $Cp^*_2YbL_n$ complexes. A $^1H/^{171}Yb$ HMQC spectrum of **7** at -7 °C,[53] optimized for this J_{YbH} value, gives a ^{171}Yb resonance (at +139 ppm) that is correlated to the Cp^* protons. A similar experiment gives a ^{171}Yb resonance at +140 ppm for **12** (at -73 °C); this resonance is correlated with the $SiMe_3$ protons, indicating that long-range (4-bond) Yb-H communication is present. It appears that this method of indirectly detecting ^{171}Yb resonances, *via* long-range J_{YbH} coupling (involving either the Cp* protons or protons on the ligand, L), will be useful for any slow-exchange $Cp^*_2YbL_n$ complex.[54] The technique of using long range M-H coupling to indirectly detect M spectra with increased sensitivity has been reported previously.[55]

Table 7 lists the ^{171}Yb chemical shifts of $Cp^\#_2YbL_n$ complexes ($Cp^\#$ = any Cp derivative) that have been reported to-date.[56]

(Table 7 here)

A rough correlation of the ^{171}Yb chemical shift with coordination number can be made. Specifically, the base-free adducts Cp^*_2Yb (**1**) and $(1,3\text{-}(SiMe_3)_2C_5H_3)_2Yb$ have chemical shifts of -30 and -16 ppm, respectively. The 1:1 adducts resonate slightly downfield, from 0 to +140 ppm (with the value for $(1,3\text{-}(SiMe_3)_2C_5H_3)_2Yb(OEt_2)$ being an exception), and the 1:2 adducts have chemical shifts from +340 to +950 ppm (with the value for $Cp^*_2Yb(thf)_2$ being an exception). Several of the values were measured under fast-exchange conditions (including the values for $(1,3\text{-}(SiMe_3)_2C_5H_3)_2Yb(OEt_2)$ and $Cp^*_2Yb(thf)_2$), as noted in the Table, and so these chemical shift values are averaged values. While a dependence on coordination number is a common feature for metal chemical shifts, correlation of metal chemical shifts with specific chemical properties (as is frequently done for ^1H and ^{13}C chemical shifts) is often ambiguous.[22] The paramagnetic shielding contribution to the chemical shift, the dominant factor for metal chemical shifts, includes terms that are dependent on low-lying magnetic dipole-allowed transitions to excited states of the complex, the inverse cube of the distance of the valence p and d electrons from the metal nucleus, and the imbalance of electron distribution on the metal center.[22] In addition, relativistic effects on ^{171}Yb chemical shifts will be significant.[57] These factors are not well-understood for many metals,[55a,58] and certainly not for $Cp^*_2YbL_n$ complexes; consequently, information contained within ^{171}Yb chemical shifts remains a mystery.

Conclusions

The interactions of **1** with phosphines have been found to have relatively high kinetic barriers, allowing investigation of the solution-state perturbations that result from such interactions. Both 1:1 and 1:2 adducts can be isolated; $^1J_{YbP}$ is significantly reduced for the 1:2 adducts, relative to the 1:1 adducts. The presence of >2 eq. of phosphine results in faster (associative) intermolecular exchange, a common feature of $Cp^*_2YbL_n$

systems.[7] The barrier to intermolecular exchange for phosphine oxide and imine adducts is much higher, and these adducts undergo slow exchange at 25 °C. Both 1:1 and 1:2 adducts can be isolated for these derivatives also, however the latter are insoluble in hydrocarbon and aromatic solvents. The $^2J_{YbP}$ values for the 1:1 adducts are an order of magnitude less than the analogous one-bond values for the phosphine derivatives. While an adduct with the unsymmetrical ylide $Me_2PhPCHSiMe_3$ undergoes fast intermolecular exchange at 25 °C, this exchange can be slowed at low temperature. An intramolecular process, resulting in equivalent P<u>Me2</u> groups and equivalent Cp^* rings, can also be slowed at a lower temperature; possible mechanisms for this process have been discussed.

We are continuing our investigations of the solution- and solid-state perturbations that result from the interactions of **1** with various nonclassical Lewis bases. As above, the NMR-active ^{171}Yb isotope will be utilized in these studies. Our focus remains on slow-exchange adducts, for which J_{YbX} values can be measured to give information concerning the nature of the Lewis acid-base interactions in the solution state. The results of these investigations will be reported at a later date.

Experimental Details

General Comments. All reactions and product manipulations were carried out under dry nitrogen using standard Schlenk and dry box techniques. Solvents and reagents were dried and purified as described previously.[59] Infrared spectra, melting points, elemental analyses, and the NMR spectra were obtained as previously described.[59]

^{1}H NMR shifts are relative to tetramethylsilane; the residual solvent peak was used as an internal reference. $^{31}P\{^1H\}$ NMR shifts are relative to 85% H_3PO_4 at δ 0.0, with shifts downfield of the reference considered positive. ^{171}Yb shifts are referenced to an absolute frequency scale relative to the reported frequency of $Cp^*_2Yb(thf)_2$,[56b] and scaled according to the ^{1}H frequency of the particular machine used. In all cases where ^{171}Yb chemical shifts were being investigated, the HMQC pulse sequence was used,[14] and first a large sweep width in the ^{171}Yb dimension was used, followed by a smaller sweep width, to assure that the resonance was not folded. The HMQC pulse sequence was also used to acquire $^1H/^{13}C$ spectra (to obtain the ^{13}C NMR data for **12**, **13**). The $^1J_{CH}$ values for **12**, **13**, and the free ylides, were obtained from ^{13}C-filtered ^{1}H spectra, using the standard Bruker pulse sequence, with optimized 90° pulses and delays.

$Cp^*_2Yb(PMe_3)_2$ (2). Trimethylphosphine (0.086 mL, 0.84 mmol) was added dropwise to a solution of **1** (0.18 g, 0.41 mmol) in toluene (15 mL). The solution turned bright green and a dark green crystalline solid precipitated from solution within minutes. The mixture was slowly cooled to -80 °C, yielding the product as dark green crystals (0.22 g, 88%), mp 110 °C (decomp. to a black solid). ^{1}H NMR (C_6D_6): δ 2.05 (s, 30H), 0.76 (s, 18H). $^{31}P\{^1H\}$ NMR (C_6D_6): δ -55.8 (s) ppm. IR: 2718 m, 1377 s, 1367 m, 1326 w, 1304 s, 1281 m, 1017 m, 960 s, 939 s, 839 w, 801 w, 722 m, 710 m, 668 w, 663 w, 624 w, 591 m cm^{-1}. Anal. Calcd for $C_{26}H_{48}P_2Yb$: C, 52.4; H, 8.12. Found: C, 52.3; H, 8.30.

$Cp^*_2Yb(PEt_3)$ (3). Triethylphosphine (0.060 mL, 0.40 mmol) was added dropwise to a toluene solution (15 mL) of **1** (0.12 g, 0.27 mmol). The resulting dark blue solution was concentrated to *ca.* 10 mL. Slow cooling to -80 °C yielded the product as dark blue crystals (0.10 g, 66%), mp 128 °C (decomp. to a dark brown oil). ^1H NMR (C_6D_6): δ 2.04 (s, 30H), 1.27 (6H, qd, $^3J_{HH}$ = 7.6 Hz, $^2J_{PH}$ = 1.6 Hz), 0.77 (9H, dt, $^3J_{PH}$ = 14.4 Hz, $^3J_{HH}$ = 7.6 Hz). $^{31}P\{^1H\}$ NMR (C_6D_6): δ -12.6 (s) ppm. IR: 2721 m, 1417 m, 1377 s, 1262 s, 1098 s, 1036 s, 1023 s, 865 w, 803 s, 766 m, 756 m, 702 m, 672 w, 622 w, 590 w cm^{-1}. Anal. Calcd for $C_{26}H_{48}P_2Yb$: C, 55.6; H, 8.08. Found: C, 55.5; H, 8.13.

$Cp^*_2Yb(1,2\text{-}(Me_2P)_2C_6H_4)$ (6). To a toluene solution (15 mL) of **1** (0.15 g, 0.34 mmol), 1,2-$(Me_2P)_2C_6H_4$ (0.056 mL) was added dropwise. The resulting dark green-brown solution was concentrated to *ca.* 10 mL, and then filtered. Slow cooling to -40 °C yielded the product as maroon crystals (0.10 g, 46%), mp the compound did not melt sharply but darkened to a brown oil over the temperature range 260-290 °C. ^1H NMR (C_6D_6): δ 7.11 (m, 2H), 7.04 (m, 2H), 2.06 (s, 30H), 1.03 (s, 12H). $^{31}P\{^1H\}$ NMR (C_6D_6): δ -42.5 (s, $w_{1/2}$ = 40 Hz (see text), $^1J_{YbP}$ = 650 Hz) ppm. IR: 2720 m, 1426 s, 1376 s, 1299 s, 1283 w, 1277 w, 1134 w, 1119 m, 1018 w, 942 s, 907 s, 874 m, 827 w, 799 w, 753 s, 730 m, 718 m, 686 w, 677 w, 589 w, 463 m, 452 w cm^{-1}. Anal. Calcd for $C_{30}H_{46}P_2Yb$: C, 56.2; H, 7.23. Found: C, 56.3; H, 7.39.

$Cp^*_2Yb(OPMe_3)$ (7). A toluene solution (10 mL) of Me_3PO (0.040 g, 0.44 mmol) was added dropwise to a stirred solution of **1** (0.19 g, 0.43 mmol) in toluene (10 mL). The solution turned orange near the end of the addition. The solvent was removed under reduced pressure, giving the crude product as a yellow-orange solid. This solid was washed with pentane (2 x 20 mL) and dried under reduced pressure, giving the product as a fine yellow powder (0.19 g, 83%), mp 303-307 °C (decomp.). ^1H NMR (C_6D_6): δ 2.14 (s, 30H), 0.65 (d, 9H, $^2J_{PH}$ = 12.8 Hz) ppm. $^{31}P\{^1H\}$ NMR (C_6D_6): δ 45.6 (s, $^2J_{YbP}$ =

95 Hz) ppm. IR: 2720 m, 1417 m, 1377 m, 1344 w, 1309 s, 1296 s, 1154 s, 1108 w, 1022 w, 945 s, 857 s, 799 w, 747 m cm^{-1}. Anal. Calcd for $C_{23}H_{39}OPYb$: C, 51.6; H, 7.34. Found: C, 51.7; H, 7.08.

$Cp^*_2Yb(OPMe_3)_2$ (8). A toluene solution (10 mL) of Me_3PO (0.070 g, 0.76 mmol) was added dropwise to a toluene solution (10 mL) of **1** (0.15 g, 0.34 mmol). An orange solid precipitated from the solution during the addition. The solid was allowed to settle, the solvent was removed *via* cannulation, and the solid was washed with toluene (2 x 10 mL). Drying under reduced pressure yielded the product as a pumpkin-colored solid (0.080 g, 38%), mp 290 °C (decomp. to a red-brown oil). ^1H NMR (thf-d_8): δ 1.85 (s, 15H, $w_{1/2}$ = 1 Hz), 1.53 (broad s, 9H, $w_{1/2}$ = 38 Hz, see text). $^{31}P\{^1H\}$ NMR (thf-d_8): δ 39.3 (broad s, $w_{1/2}$ = 480 Hz, see text) ppm. Free Me_3PO in thf-d_8 has the following values, ^1H NMR: 1.34 (d, $^2J_{PH}$ = 12.8 Hz) ppm; $^{31}P\{^1H\}$ NMR: 30.5 (s) ppm. IR: 2717 w, 1377 m, 1344 w, 1308 s, 1295 s, 1182 s, 1166 s, 1021 w, 944 s, 861 m, 798 w, 750 m, 721 w cm^{-1}. A satisfactory elemental analysis was not obtained on this sample, since it was difficult to find a suitable crystallization solvent, see text. (the procedure used above gave a product that was consistently *ca.* 1% low in carbon).

$Cp^*_2Yb(HNPEt_3)$ (9). A toluene solution (10 mL) of Et_3PNH[60] (0.045 g, 0.34 mmol) was added dropwise to a toluene solution (10 mL) of **1** (0.15 g, 0.34 mmol). The resulting orange solution was stirred for 30 min and filtered. Slow cooling of the solution to -80 °C gave the product as a fine light orange powder (0.10 g, 51 %), mp 240 °C (decomp. to a dark brown oil). ^1H NMR (toluene-d_8): δ 2.12 (s, 30H), 1.20 (dq, 6H, $^2J_{PH}$ = 12.1 Hz, $^3J_{HH}$ = 7.8 Hz), 0.61 (dt, 9H, $^3J_{PH}$ = 16.8 Hz, $^3J_{HH}$ = 7.8 Hz) ppm (the N-H resonance is not observed, see text). $^{31}P\{^1H\}$ NMR (toluene-d_8): δ 60.1 (s, $^2J_{YbP}$ = 92 Hz) ppm. IR: 2721 m, 1412 m, 1379 s, 1283 m, 1264 m, 1139 s, 1046 m, 1027 m,

1012 m, 983 w, 783 s, 769 s, 741 w, 724 m cm^{-1}. Anal. Calcd for $C_{26}H_{46}NPYb$: C, 54.2; H, 8.04. Found: C, 54.4; H, 7.76.

$Cp^*_2Yb(Me_2PhPCHSiMe_3)$ (12). To a stirred solution of **1** (0.12 g, 0.34 mmol) in toluene (10 mL), $Me_2PhPCHSiMe_3$[30] (0.061 mL) was added dropwise. The resulting dark green solution was filtered, and slowly cooled to -40 °C, yielding the product as dark green crystals (0.10 g, 55%) , mp 103 °C (decomp). ^1H NMR (toluene-d_8): δ 7.4-7.0 (m, 5H), 2.14 (s, 30H), 1.22 (d, 6H, $^2J_{PH}$ = 12.5 Hz), 0.24 (d, 1H, $^2J_{PH}$ = 20.5 Hz), 0.16 (s, 9H) ppm. $^{31}P\{^1H\}$ NMR (toluene-d_8): δ 10.8 (s) ppm. IR: 1420 m, 1378 m, 1329 w, 1310 w, 1301 m, 1288 m, 1254 m, 1244 m, 1163 w, 1123 s, 1105 m, 1076 w, 1016 w, 958 s, 922 s, 917 s, 856 s, 832 s, 767 m, 747 s, 723 w, 697 m, 681 m, 639 m, 590 m, 491 m, 421 m cm^{-1}. Anal. Calcd for $C_{32}H_{51}PSiYb$: C, 57.6; H, 7.70. Found: C, 57.6; H, 8.0.

$Cp^*_2Yb(Me_2PhPCH_2)$ (13). To a stirred solution of **1** (0.15 g, 0.34 mmol) in toluene (10 mL), Me_2PhPCH_2[30] (0.047 mL) was added dropwise. The resulting dark maroon solution was slowly cooled to -80 °C, yielding the product as reddish-brown crystals (0.16 g, 79%), mp 166-178 °C. ^1H NMR (toluene-d_8): δ 7.2-6.95 (m, 5H), 2.06 (s, 30H), 1.05 (d, 6H, $^2J_{PH}$ = 12.8 Hz), -0.20 (d, 2H, $^2J_{PH}$ = 13.4 Hz) ppm. $^{31}P\{^1H\}$ NMR (toluene-d_8): δ 18.7 (s) ppm. IR: 2721 m, 1437 s, 1420 m, 1378 m, 1367 m, 1304 m, 1289 w, 1262 w, 1182 w, 1159 m, 1113 m, 1018 m, 1000 w, 977 m, 953 s, 925 s, 844 m, 819 w, 799 w, 760 m, 744 s, 725 s, 692 s, 667 m, 494 m, 419 m cm^{-1}. Anal. Calcd for $C_{29}H_{73}PYb$: C, 58.5; H, 7.29. Found: C, 58.2; H, 7.36.

X-ray Structure Determination of 12.

X-ray quality crystals of **12** were grown as described above. The crystals were placed in Paratone N oil, mounted on the end of a cut quartz capillary tube, and placed under a flow of cold nitrogen on an Enraf-Nonius CAD4 diffractometer. Crystal data and numerical details of the structure determination are given in Tables 4-6. Intensities were collected with graphite-monochromatized MoKα (λ = 0.71073 Å) radiation using the θ-2θ scan technique. Lattice parameters were determined using automatic peak search and indexing procedures. Intensity standards were measured every hour of data collection.

The raw intensity data were converted to structure factor amplitudes and their esds by correction for scan speed, background, and Lorentz and polarization effects. Correction for crystal decomposition was not necessary. Analysis of the data, collected based on a triclinic unit cell, suggested a C-centered monoclinic lattice. A θ-independent differential absorption (DIFABS) correction[37] was applied to the raw data, using an isotropic model in the space group P1 as a basis for the correction (the Yb atoms were found using Patterson techniques; the non-hydrogen atoms were located using standard least-squares and Fourier techniques;[61,62] and hydrogens were included in this model, in positions assuming idealized bonding geometry about the carbon atoms).

The absorption-corrected data were transformed to a C-centered monoclinic unit cell, and the atomic positions were transformed to the space group Cc. The systematic absences were rejected, and the redundant data were averaged (R_{int} = 0.077). The carbon atoms were refined isotropically, the heavy atoms were refined anisotropically, and no hydrogen atoms were included in the final model. The enantiomorph that gave the best agreement with the data was used. Attempts to refine the carbon atoms anisotropically resulted in irrational thermal parameter values (non-positive definite tensors), for many of these atoms.

The least-squares program minimized the expression, $\Sigma w(|F_o| - |F_c|)^2$, where w is the weight of a given observation. A value of 0.05 for the p-factor was used to reduce

the weight of intense reflections in the refinements. The analytical forms of the scattering factor tables for the neutral atoms were used[63a] and all non-hydrogen scattering factors were corrected for both real and imaginary components of anomalous dispersion.[63b]

References.

(1) (a) Brookhart, M.; Green, M. L. H.; Wong, L. L. *Prog. Inorg. Chem.* **1988**, *36*, 1. (b) Arndsten, B. A.; Bergman, R. G.; Mobley, T. A.; Peterson, T. H. *Acc. Chem. Res.* **1995**, *28*, 154.

(2) (a) Jordan, R. F. *Adv. Organomet. Chem.* **1991**, *32*, 325. (b) Cossee, P. *J. Catal.* **1964**, *3*, 80. (c) Arlman, E. J.; Cossee, P. *J. Catal.* **1964**, *3*, 99. (d) Leclerc, M. K.; Brintzinger, H. H. *J. Am. Chem. Soc.* **1995**, *117*, 1651.

(3) (a) Andersen, R. A.; Boncella, J. M.; Burns, C. J.; Green, J. C.; Hohl, D.; Rosch, N. *J. Chem. Soc., Chem. Commun.* **1986**, 405. (b) Andersen, R. A.; Boncella, J. M.; Burns, C. J.; Blom, R.; Haaland, A.; Volden, H. V. *J. Organomet. Chem.* **1986**, *312*, C49. (c) Andersen, R. A.; Blom, R.; Boncella, J. M.; Burns, C. J.; Volden, H. V. *Acta Chem. Scand.* **1987**, *A41*, 24. (d) Green, J. C.; Hohl, D.; Rosch, N. *Organometallics.* **1987**, *6*, 712.

(4) (a) Burns, C. J.; Andersen, R. A. *J. Am. Chem. Soc.* **1987**, *109*, 941. (b) Burns, C. J.; Andersen, R. A. *J. Am. Chem. Soc.* **1987**, *109*, 5853. (c) Burns, C. J.; Andersen, R. A. *J. Am. Chem. Soc.* **1987**, *109*, 915.

(5) Schumann, H.; Glanz, M.; Winterfeld, J.; Hemling, H.; Kuhn, N.; Kratz, T. *Angew. Chem., Int. Ed. Engl.* **1994**, *33*, 1733.

(6) The paramagnetic shift induced by Cp^*_2Eu has been used to study weak metal-ligand bonding in an indirect way: Nolan, S. P.; Marks, T. J. *J. Am. Chem. Soc.* **1989**, *111*, 8538.

(7) Schwartz, D. J.; Ball, G. E.; Andersen, R. A. *J. Am. Chem. Soc.*, in press.

(8) (a) Hitchcock, P. B.; Holmes, S. A.; Lappert, M. F.; Tian, S. *J. Chem. Soc., Chem. Commun.* **1994**, 2691. (b) Tilley, T. D.; Andersen, R. A.; Zalkin, A. *Inorg. Chem.* **1983**, *22*, 856. (c) Tilley, T. D.; Andersen, R. A.; Zalkin, A. *J. Am. Chem. Soc.* **1982**, *104*, 3725. (d) Brennan, J. G.; Stults, S. D.; Andersen, R. A.; Zalkin, A. *Organometallics.* **1988**, *7*, 1329, and references therein. (e) Schlesener, C. J.; Ellis, A. B.

Organometallics. **1983**, *2*, 529. (f) Brennan, J. G.; Andersen, R. A.; Robbins, J. L. *J. Am. Chem. Soc.* **1986**, *108*, 335. (g) Hitchcock, P. B.; Lappert, M. F.; MacKinnon, I. A. *J. Chem. Soc., Chem. Commun.* **1988**, 1557. (h) Fryzuk, M. D.; Haddad, T. S. *J. Chem. Soc., Chem. Commun.* **1990**, 1088.

(9) All coalescence temperatures given in the text were measured at 300 MHz ^1H frequency, and were measured on samples containing 1 eq. excess of **1**. These values may be used as a qualitative measure of the kinetic barrier to intermolecular exchange.

(10) The exchange rate is faster for samples containing excess phosphine, relative to samples containing a slight excess of **1**. Consequently, all stopped-exchange NMR values reported in the text were measured on samples containing *ca.* 1 eq. excess of **1**. It has been found that the number of excess equivalents of **1** present has no effect on the exchange rate; i.e., the exchange mechanism in the presence of excess **1** is dissociative.[7]

(11) Bryant, R. G. *J. Chem. Ed.* **1983**, *60*, 933.

(12) The recently-reported [$Yb(CH(SiMe_3)_2)_2(dmpe)$] complex[8a] is soluble in toluene; only the exchange-averaged room temperature NMR data were reported.

(13) This coupling is likely unresolved for complexes **2-4** as a result of the broader resonances present at the low temperatures required to slow intermolecular exchange in these systems.

(14) (a) Bax, A.; Griffey, R. H.; Hawkins, B. L. *J. Magn. Reson.* **1983**, *55*, 301. (b) Bax, A.; Subramanian, S. *J. Magn. Reson.* **1986**, *67*, 565.

(15) The solid-state structure of $Cp^*_2Yb(OEt_2)$ has a γ-CH_3 interaction involving the methyl group of the diethyl ether ligand: P. L. Watson, personal communication.

(16) Agostic complexes with unchanged $^1J_{CH}$ values are known, see ref. 7 and: (a) Neve, F.; Ghedini, M.; Crispini, A. *Organometallics*. **1992**, *11*, 3324. (b) Albinati, A.; Pregosin, P. S.; Wombacher, F. *Inorg. Chem.* **1990**, *29*, 1812. (c) Albinati, A.; Anklin, C. G.; Ganazoli, F.; Ruegg, H.; Pregosin, P. S. *Inorg. Chem.* **1987**, *26*, 503.

(17) This assumes that the hybridization of the ^{31}P and ^{171}Yb nuclei are the same in both the 1:1 and the 1:2 adducts, see ref. 22, Ch. 4.

(18) While chelation does not appear to affect the enthalpic strength of the Yb-P interactions, based on the NMR data, it does have an affect on the entropic contribution to the ΔG(interaction) value, as mentioned in the Discussion section.

(19) Reaction of $Cp^*_2Yb(OEt_2)$ with Ph_3PS gives $[Cp^*_2Yb(\mu\text{-}S)]_2$.[20] Apparently, the base-free derivative **1** also reacts similarly, as a resonance for free Ph_3P becomes visible in the $^{31}P\{^1H\}$ spectrum of this sample over the course of several hours.

(20) Berg, D. J.; Burns, C. J.; Andersen, R. A.; Zalkin, A. *Organometallics*. **1989**, *8*, 1865.

(21) Tilley, T. D.; Andersen, R. A.; Spencer, B.; Ruben, H.; Zalkin, A.; Templeton, D. H. *Inorg. Chem.* **1980**, *19*, 2999.

(22) Jameson, C. J.; Mason, J. In *Multinuclear NMR*; Mason, J., Ed.; Plenum Press: New York, 1987; Ch. 3.

(23) Birkofer, L.; Kim, S. M. *Chem. Ber.* **1964**, *97*, 2100.

(24) Dixon, D. A. In *Ylides and Imines of Phosphorus*, Johnson, A. W., Ed.; John Wiley & Sons, Inc.: New York, 1993; Ch. 2.

(25) Gilheany, D. G. *Chem. Rev.* **1994**, *94*, 1339.

(26) Kaska, W. C. *Coord. Chem. Rev.* **1983**, *48*, 1.

(27) Starzewski, K. A. O.; Feigel, M. *J. Organomet. Chem.* **1975**, *93*, C20.

(28) Liu, Z.-p.; Schlosser, M. *Tet. Letters*. **1990**, *31*, 5753.

(29) Grim, S. O. In *Phosphorus-31 NMR Spectroscopy in Stereochemical Analysis: Organic Compounds and Metal Complexes*, Verkade, J. G. and Quin, L. D., eds.; VCH Publishers: Deerfield Beach, FL, 1987; Ch. 18.

(30) Schmidbaur, H.; Heimann, M. *Z. Naturforsch.* **1978**, *29b*, 485.

(31) These temperatures were chosen as they are well below the T_c(intermolecular exchange) temperatures.

(32) The ^{31}P chemical shift of ylides nearly always shifts downfield upon coordination to a metal, see ref. 29.

(33) (a) Schumann, H.; Reier, F. W.; Dettlaff, M. *J. Organomet. Chem.* **1983**, *255*, 305. (b) Werner, H.; Schippel, O.; Wolf, J.; Schulz, M. *J. Organomet. Chem.* **1991**, *417*, 149.

(34) Several $^{1}H/^{13}C$ HMQC spectra were obtained on a sample of **12** at -78 °C, however Yb-C or Yb-H coupling was not resolved in any of them. A $^{1}J_{YbC}$ value of 0.32 Hz has recently been reported for $\{Yb[N(SiMe_3)C(tBu)CH(SiMe_3)]_2\}$.[8a] This value is unexpectedly small, considering the $^{1}J_{YbC}$ value of 48 Hz that we have found for $(dippe)Pt(\mu\text{-}CH_3)(\mu\text{-}H)YbCp^*_2$.[7] The $^{1}J_{YbC}$ value for $Yb[C(SiMe_3)_3]_2$ was not reported.[35]

(35) Eaborn, C.; Hitchcock, P. B.; Izod, K.; Smith, J. D. *J. Am. Chem. Soc.* **1994**, *116*, 12071.

(36) (a) Schumann, H.; Albrecht, I.; Reier, F.-W.; Hahn, E. *Angew. Chem., Int. Ed. Engl.* **1984**, *23*, 522. (b) Wong, W.-K.; Guan, J.; Ren, J.; Shen, Q.; Wong, W.-T. *Polyhedron.* **1993**, *12*, 2749. (c) Wong, W.-K.; Guan, J. W.; Shen, Q.; Zhang, L. L.; Lin, Y.; Wong, W.-T. *Polyhedron.* **1995**, *14*, 277.

(37) Walker, N.; Stuart, D. *Acta Crystallogr.* **1983**, *A39*, 158.

(38) A P=C double bond distance is 1.665 Å,[25] and a P-C single bond distance is 1.872 Å.[24]

(39) Pauling, L. In *The Nature of the Chemical Bond, 3rd ed.*; Cornell University Press: Ithaca, New York, 1960; pp. 260-261.

(40) Such a $\gamma\text{-}CH_3$ interaction involving the methyl of an $SiMe_3$ group and Yb has been reported for $Yb[(N(SiMe_3)_2]_2(dmpe)$.[8c]

(41) (a) Marder, T. B.; Fultz, W. C.; Calabrese, J. C.; Harlow, R.; Milstein, D. *J. Chem. Soc., Chem. Commun.* **1987**, 1543. (b) Kermode, N. J.; Lappert, M. F.; Skelton, B.

W.; White, A. H.; Holton, J. *J. Organomet. Chem.* **1982**, *228*, C71; and references therein. (c) Buchanan, R. M.; Pierpont, C. G. *Inorg. Chem.* **1979**, *18*, 3608.

(42) The bent geometry of **1** and the overall lack of structural changes upon forming Lewis acid-base adducts with **1** results in the expectation that the kinetic barrier to exchange will serve as a qualitative indicator of the thermodynamic strength of the interaction.

(43) (a) Nief, F.; Ricard, L.; Mathey, F. *Polyhedron.* **1993**, *12*, 19. (b) Karsch, H. H.; Ferazin, G.; Steigelmann, O.; Kooijman, H.; Hiller, W. *Angew. Chem., Int. Ed. Engl.* **1993**, *32*, 1739. (c) Fryzuk, M. D.; Haddad, T. S.; Berg, D. J. *Coord. Chem. Rev.* **1990**, *90*, 137.

(44) The reduced coupling constant is given by: $K = (4\pi^2 J_{AB})/(H\gamma_A\gamma_B)$; all values given in the text are to the 10^{20} power, and are in $NA^{-2}m^{-3}$ units.

(45) Blaschke, G.; Schmidbaur, H.; Kaska, W. C. *J. Organomet. Chem.* **1979**, *182*, 251.

(46) Feser, R.; Werner, H. *Angew. Chem., Int. Ed. Engl.* **1980**, *19*, 940.

(47) Movement of the ylide molecule relative to **1** is identical to movement of **1** relative to the ylide molecule. For clarity, the latter frame of reference will be used for the discussion. Also, while rotation of the C(H)($SiMe_3$) moiety about the P-C bond may be occurring (the barrier to rotation about P-C ylide bonds is small),[28] this would not have a significant effect on the process under discussion.

(48) Peng, T.-S.; Gladysz, J. A. *J. Am. Chem. Soc.* **1992**, *114*, 4174.

(49) Similar interactions involving an olefinic C-H bond have been proposed to explain kinetic and isotopic effects in the $Cp^*Ir(PMe_3)(C_2H_4)$ system: (a) Stoutland, P. O.; Bergman, R. G. *J. Am. Chem. Soc.* **1985**, *107*, 4581. (b) Stoutland, P. O.; Bergman, R. G. *J. Am. Chem. Soc.* **1988**, *110*, 5732.

(50) See ref. 48 for a more thorough discussion on this topic.

(51) Elser, V. H.; Dreeskamp, H. *Ber. Bunsenges. Phys. Chem.* **1969**, *73*, 619.

(52) Crabtree, R. H. *Angew. Chem., Int. Ed. Engl.* **1993**, *32*, 789. While certain agostic complexes have $^1J_{CH}$ values that are relatively unchanged from the "free" $^1J_{CH}$ values, this is usually[16] a result of averaging of a smaller agostic $^1J_{CH}$ value with larger, unperturbed $^1J_{CH}$ values; this is not possible for **12**.

(53) Slight exchange broadening of the Cp* resonances is present in the 25 °C ^1H spectrum.

(54) The potential of this technique for other $Cp^{\#}ML_n$ complexes ($Cp^{\#}$ = a Cp derivative; M = an NMR-active metal nucleus) is currently being explored: G. E. Ball, work in progress.

(55) (a) Macchioni, A.; Pregosin, P. S.; Ruegger, H.; Koten, G. v.; van der Schaaf, P. A.; Abbenhuis, R. A. T. M. *Magn. Res. Chem.* **1994**, *32*, 235. (b) Bonny, A.; McMaster, A. D.; Stobart, S. R. *Inorg. Chem.* **1978**, *4*, 935. (c) Benn, R.; Brevard, C. *J. Am. Chem. Soc.* **1986**, *108*, 5622. (d) Benn, R.; Brenneke, H.; Joussen, E.; Lehmkuhl, H.; Lopez Ortiz, F. *Organometallics*. **1990**, *9*, 756.

(56) (a) Hitchcock, P. B.; Howard, J. A. K.; Lappert, M. F.; Prashar, S. *J. Organomet. Chem.* **1992**, *437*, 177. (b) Avent, A. G.; Edelman, M. A.; Lappert, M. F.; Lawless, G. A. *J. Am. Chem. Soc.* **1989**, *111*, 3423. (c) Nief, F.; Ricard, L.; Mathey, F. *Polyhedron*. **1993**, *12*, 19. (d) van den Hende, J. R.; Hitchcock, P. B.; Lappert, M. F. *J. Organomet. Chem.* **1994**, *472*, 79.

(57) Mason, J. *Chem. Rev.* **1987**, *87*, 1299.

(58) Pregosin, P. S. In *Annual Reports on NMR Spectroscopy, Vol. 17*; Webb, G. A., ed.; Academic Press Inc.: London, 1986.

(59) Schwartz, D. J.; Andersen, R. A. *J. Am. Chem. Soc.* **1995**, *117*, 4014.

(60) Birkofer, L.; Kim, S. M. *Chem. Ber.* **1964**, *97*, 2100. This compound was obtained as a crystalline white solid, crystallized from diethyl ether, in contrast to a colorless oil as reported.

(61) All calculations were performed on a DEC Microvax II or a DEC Microvax 4000 using locally modified Nonius-SDP software operating under Micro-VMS operating system.

(62) (a) Frenz, B. A. In *Structure Determination Package Users Guide*; Texas A & M University and Enraf-Nonius: College Station, TX and The Netherlands, 1985. (b) Fair, C. K. In *MolEN Molecular Structure Solution Procedures*; Enraf-Nonius, Delft Instruments, X-ray Diffraction B. V.: The Netherlands, 1990.

(63) (a) Cromer, D. T.; Waber, J. T. In *International Tables for X-ray Crystallography, Vol. IV*; The Kynoch Press: Birmingham, England, 1974; Table 2.2B. (b) Cromer, D. T., *ibid.*, Table 2.3.1.

Acknowledgment. This work was supported by the Director, Office of Energy Research, Office of Basic Energy Sciences, Chemical Sciences Division of the U.S. Department of Energy under Contract No. DE-AC03-76F00098. We thank the National Science Foundation for a predoctoral fellowship to DJS; Dr. Graham E. Ball for helpful discussions, including the idea of using long-range J_{YbH} coupling from the Cp^* methyl groups of $Cp^*_2YbL_n$ complexes to indirectly detect ^{171}Yb spectra; Mr. Christopher D. Tagge for helpful discussions; and Dr. F. J. Hollander for helpful advice concerning X-ray crystallography.

Supplementary Material Available: Complete table of bond lengths and angles (12 pp.), anisotropic thermal parameters (1 page), root mean square amplitudes of thermal vibration (1 page), and observed and calculated structure factors (13 pp.), for **12**. This material is contained in many libraries on microfiche, immediately follows this article in the microfilm version of the journal, can be ordered from the ACS and can be downloaded from the Internet; see any current masthead page for ordering information and Internet access instructions.

TABLES

Table 1. Low Temperature ^{1}H, ^{31}P NMR Data for Phosphine Adducts of **1** (toluene-d_8).[a]

Sample	Temp. (°C)	δ(P)	$^{1}J_{YbP}$	δ(Cp*)[b]	δ(H)
PMe_3	-93	-62.0	---	---	0.78
1:2 adduct, **2**	-101	-49.2	600(20)[c]	2.28	0.64
1:1 adduct, **4**[d]	-93	-45.4	956	2.20	0.54
PEt_3	-93	-23.0	---	---	1.02 (Me), 1.18 (CH_2)
1:1 adduct, **3**	-103	-3.7	950	2.24	0.51 (Me), 1.15 (CH_2)
1 + xs PEt_3	-103	-16.3[e]	not resolved	2.24	0.80 (Me), 1.16 (CH_2)
dmpm	-65	-57.1	---	---	not measured
5	-65	-35.6	580	2.27	not measured
1,2-$(PMe_2)_2C_6H_4$	-20	-52.9	---	---	1.18
6[f]	-20	-38.4	656	2.06	1.02

[a]For this and all other Tables, chemical shift values are given in ppm, and coupling constants are given in Hz.

[b]As mentioned in the text, many of the samples were made with a slight excess of **1**, to minimize intermolecular exchange; consequently, a free Cp* resonance at *ca.* 2.00 ppm was also present for these low temperature samples.

[c]For this and all other Tables containing NMR data, estimated experimental uncertainties are given in parentheses, for values where the uncertainty is relatively large.

[d]Values given were measured from a sample containing 0.8 eq. PMe_3/1 eq. **1**, see text.

[e]The half height width of this resonance is *ca.* 900 Hz, see text.

[f]In addition, a $^{3}J_{YbPCH3}$ of 2.7 Hz was resolved, see text.

Table 2. ^{1}H, ^{31}P NMR Values for Phosphine Oxide and Imine Complexes of **1**.

Sample	Temp. (°C)	δ(P)	$^{2}J_{YbP}$	δ(Cp*)	δ(H)
Me_3PO	25	29.4	---		0.83[a]
7	25	45.6	94.6	2.14	0.65
Et_3PNH	25	44.6	---	---	1.15 (CH_2)
					0.86 (Me)
9[b]	25	60.1	91.6	2.12	1.20 (CH_2)
					0.61 (Me)
$Et_3PNSiMe_3$[b]	-83	18.2	---	---	1.00 (CH_2)
					0.79 (Me)
					0.42 ($SiMe_3$)
11[b]	-83	33.6	7(1)	2.34	1.22 (CH_2)
					0.47 (Me)
					0.18 ($SiMe_3$)

[a]The $^{2}J_{PH}$ values for Me_3PO and **7** are identical, 12.8 Hz.

[b]These samples in toluene-d_8, the others in C_6D_6.

Table 3. Low Temperature ^{1}H, ^{13}C, ^{31}P NMR Values for the Phosphine Ylide Complexes **12** and **13**.[a]

Value[b]	$Me_2PhPCHSiMe_3$	**12**[c]	Me_2PhPCH_2	**13**[c]
$\delta(Cp^*)$	---	2.31	---	2.27
$\delta(C\underline{H})/^{2}J_{PH}$	-0.30/8.7	0.39/20.3	0.37/5.3	-0.28/12.6
$\delta(C\underline{H}_3)/^{2}J_{PH}$	1.05/12.6	0.94/11.9	1.16/12.8	0.65/12.6
$\delta(Si(C\underline{H}_3)_3)$	0.50	0.20	---	---
$^{1}J_{CH}$ (C-H)	136(1)	111(2)	150(1)	119(2)
$^{1}J_{CH}$ (Me)	128(1)	129(1)	128(1)	129(1)
$^{1}J_{CH}$ ($SiMe_3$)	116(1)	116(1)	---	---
$\delta(P)$	4.6	14.4	5.1	20.0
$^{2}J_{YbP}$	---	8(1)	---	37(1)
$\delta(\underline{C}H)/^{1}J_{PC}$	-4.2/94	-2.5/53(2)	-6.1/92	-1.0/42(2)
$\delta(\underline{C}H_3)/^{1}J_{PC}$	16.9/63	18.0/65(2)	15.7/67	15.1/62(2)
$\delta(Si(\underline{C}H_3)_3)/^{3}J_{PC}$	4.9/4.2	3.5/unresolved	---	---

[a]The values for $Me_2PhPCHSiMe_3$ and **12** were acquired at -78 °C. The values for Me_2PhPCH_2 and **13** were acquired at -93 °C.

[b]All of these values were obtained from typical 1-D direct-detected spectra, with the exceptions of the $^{1}J_{CH}$ values (obtained from ^{13}C-filtered ^{1}H spectra) and the $\delta(C)$, J_{PC} values for **12** and **13** (obtained from $^{1}H/^{13}C$ HMQC 2-D spectra). See the Experimental section for details.

[c]These samples contained 1 eq. excess of **1**.

Table 4. Crystallographic Data for $Cp^*_2Yb(Me_2PhPCHSiMe_3)$, **12.**

chem formula	$C_{32}H_{51}PSiYb$
mol wt.	667.86
crystal size (mm)	0.54 x 0.43 x 0.22
T, °C	-100
space group	Cc (#9)
a, Å	14.776(8)
b, Å	14.852(8)
c, Å	15.186(9)
β, (deg)	104.80(4)
V, Å^3	3222(3)
Z	4
d (calc.), g cm^{-3}	1.377
μ (calc.), cm^{-1}	30.0
rflns measd	±h, ±k, +l
2θ range	3-45°
no. rflns collected:	4428
absn corrm[a]	T_{max} = 1.4, T_{min} = 0.58
no. atoms in least squares	35
no. unique rflns	2305
no. rflns with $(F_o)^2 > 3\sigma(F_o)^2$	1874
p factor	0.05
no. params	154
R[b]	0.0500
R_w	0.0616
R_{all}	0.0561

GOF	1.392
diff Fourier ($e^- Å^{-3}$)	+1.01, -0.205

[a]The program DIFABS[37] was used for the absorption correction.
[b]The definitions for R and R_w are as follows:

$$R = \frac{\Sigma||F_o|-|F_c||}{\Sigma|F_o|} \qquad R_w = \sqrt{\frac{\Sigma w(|F_o|-|F_c|)^2}{\Sigma w F_o^2}}$$

Table 5. Atomic Coordinates and B Values (Å^2) for the Atoms of **12**.[a-c]

Atom	x	y	z	B(A2)
Yb	0.000	0.25898(1)	0.000	1.46(1)
P	0.0389(3)	0.3176(3)	0.2616(3)	2.14(9)
Si	-0.1565(3)	0.2527(3)	0.1488(3)	2.4(1)
C1	0.053(1)	0.090(1)	0.060(1)	1.9(3)*
C2	0.116(1)	0.121(1)	0.016(1)	2.0(3)*
C3	0.082(1)	0.127(1)	-0.073(1)	1.3(3)*
C4	-0.018(1)	0.097(1)	-0.091(1)	2.1(3)*
C5	-0.030(1)	0.076(1)	-0.005(1)	2.2(3)*
C6	0.079(1)	0.055(1)	0.161(1)	3.2(4)*
C7	0.224(1)	0.140(1)	0.065(1)	3.3(4)*
C8	0.132(1)	0.134(1)	-0.150(1)	3.5(4)*
C9	-0.092(2)	0.084(2)	-0.184(2)	4.6(5)*
C10	-0.118(2)	0.032(2)	0.006(2)	4.8(5)*
C11	-0.003(1)	0.361(1)	-0.149(1)	1.5(3)*
C12	-0.077(1)	0.395(1)	-0.114(1)	2.3(3)*
C13	-0.038(1)	0.437(1)	-0.036(1)	2.1(3)*
C14	0.063(1)	0.427(1)	-0.011(1)	1.9(3)*
C15	0.083(1)	0.382(1)	-0.085(1)	1.7(3)*
C16	-0.021(1)	0.323(1)	-0.254(2)	3.6(4)*
C17	-0.178(2)	0.399(2)	-0.169(2)	4.2(5)*
C18	-0.087(1)	0.490(1)	0.025(1)	3.2(4)*
C19	0.132(1)	0.473(1)	0.061(1)	3.0(4)*
C20	0.180(1)	0.367(1)	-0.098(2)	3.8(4)*
C21	-0.028(1)	0.267(1)	0.168(1)	1.7(3)*
C22	-0.206(1)	0.251(1)	0.024(1)	2.5(4)*
C23	-0.213(2)	0.363(1)	0.187(2)	4.0(4)*
C24	-0.193(1)	0.165(1)	0.205(1)	3.3(4)*
C25	0.015(1)	0.436(1)	0.274(1)	2.5(3)*
C26	0.163(1)	0.310(1)	0.266(1)	3.0(4)*
C27	0.035(1)	0.266(1)	0.372(1)	2.2(3)*
C28	0.012(1)	0.311(1)	0.436(1)	3.2(4)*
C29	0.017(2)	0.272(2)	0.519(2)	5.5(6)*
C30	0.033(1)	0.180(1)	0.535(2)	3.7(4)*
C31	0.054(1)	0.128(1)	0.462(1)	3.1(4)*
C32	0.051(1)	0.175(1)	0.381(1)	2.6(3)*

[a]Numbers in parentheses give estimated standard deviations. [b]Equivalent isotropic thermal parameters are calculated as $(4/3)[\alpha^2\beta_{11} + b^2\beta_{22} + c^2\beta_{33} + ab(\cos\gamma)\beta_{12} + ac(\cos\beta)\beta_{13} + bc(\cos\alpha)\beta_{23}]$. [c]Starred atoms were included with isotropic thermal parameters.

Table 6. Selected Intramolecular Distances (Å) and Angles (deg) in 12.[a]

Bond Distances			
Yb-C21	2.69(2)	Yb-Cp1	2.44
Si-C21	1.85(2)	Yb-Cp2	2.43
P-C21	1.69(2)	Yb-P	3.963(5)
Yb-C22	3.15(2)	Yb-Si	3.624(6)
Bond Angles			
Yb-C21-Si	104.6(6)	Yb-C21-P	128.4(9)
Cp1-Yb-Cp2	134.9(6)	Si-C21-P	120(1)
C21-Si-C22	106.2(9)	C21-Si-C23	116.5(9)
C21-Si-C24	111.7(8)		

[a]All distances and angles involving Cp^* rings were calculated using the ring centroid positions.

Table 7. Reported ^{171}Yb Chemical Shifts of $Cp^{\#}_2YbL_n$ Complexes ($Cp^{\#}$ = a Cp derivative).

Complex	$\delta(^{171}Yb)$, ppm	Solvent/Temp. (°C)[a]	Reference
Cp^*_2Yb, **1**[b]	-30	C_6D_6/25	this work
$(Cp^+)_2Yb$[b,c]	-16	toluene-d_8/24	56a
$(Cp^+)_2Yb(OEt_2)$[b,c,d]	-70	toluene-d_8/24	56a
$Cp^*_2Yb(OEt_2)$[d]	36	Et_2O/35	56b
$Cp^*_2Yb(thf)_2$[d]	0	thf/23	56b
$Cp^*_2Yb(NC_5H_5)_2$[d]	949	NC_5H_5/65	56b
$Cp^*_2Yb(\mu\text{-}H)_2Pt(dcype)$	572	toluene-d_8/25	7
$Cp^*_2Yb(\mu\text{-}H)_2Pt(dcypp)$	472	toluene-d_8/25	7
$Cp^*_2Yb(\mu\text{-}H)(\mu\text{-}Me)Pt(dippe)$	340	toluene-d_8/25	7
$Cp^*_2Yb(1,2\text{-}(PMe_2)C_6H_4)$, **6**	782	toluene-d_8/-30	this work
$Cp^*_2Yb(OPMe_3)$, **7**	139	toluene-d_8/-7	this work
$Cp^*_2Yb(Me_2PhPCHSiMe_3)$, **12**	140	toluene-d_8/-73	this work
$(Cp')_2Yb(thf)_2$[d,e]	242	thf/-30	56c
$(Cp'')_2Yb(thf)_2$[d,e]	316	thf/-30	56c
$(Cp^{py})_2Yb$[f]	457	C_6D_6,thf/31	56d
$(Cp'^{py})_2Yb$[f]	544	thf/31	56d
$(Cp^{py(s)})_2Yb$[f]	595	C_5D_5N/31	56d
$(Cp'^{py(s)})_2Yb$[f]	851	C_6D_6/31	56d

[a]It has been reported that ^{171}Yb chemical shifts have a significant temperature dependence.[56b]

[b]We have found some evidence for a weak interaction of **1** with aromatic solvents such as C_6D_6; consequently, these may be averaged values.

[c]$Cp^+ = 1,3\text{-}(SiMe_3)_2C_5H_3$.

[d]The ^{171}Yb chemical shifts of these complexes are likely averaged values, as fast intermolecular exchange (with solvent) is likely present for these cases.

[e]$Cp' = C_5Me_4P$; $Cp'' = C_5Me_4As$.

[f]These Cp derivatives contain a pendant pyridyl arm: $Cp^{py} = C_5H_4[C(Me)_2CH_2C_5H_4N\text{-}2]$; $Cp'^{py} = C_5H_3(SiMe_3)[\{C(Me)_2CH_2C_5H_4N\text{-}2\}\text{-}3]$; $Cp^{py(s)} = C_5H_4[C(Me)_2C_5H_4N\text{-}2]$; $Cp'^{py(s)} = C_5H_3[(SiMe_3)\{C(Me)_2C_5H_4N\text{-}2\}\text{-}3]$; see ref. 56d for details.

FIGURE CAPTIONS.

Figure 1. Examples of $Cp^{\#}_2YbL_n$ complexes ($Cp^{\#}$ = a Cp derivative) that have been crystallographically characterized.[4a,4b,5]

Figure 2. $^{31}P\{^1H\}$ spectrum of 2 at -83 °C, showing ^{171}Yb-^{31}P coupling of 956 Hz (121.5 MHz, toluene-d_8).

Figure 3. $^1H/^{171}Yb$ HMQC spectrum of **6** (300 MHz, toluene-d_8, -30 °C).

Figure 4. The two resonance structures for phosphine ylides.

Figure 5. Variable temperature ^1H spectra of **12**, with 1 eq. excess of **1** (300 MHz, toluene-d_8, -3 °C to -98 °C).

Figure 6. ORTEP diagram of $Cp^*_2Yb(Me_2PhPCHSiMe_3)$ (**13**), 50% probability thermal ellipsoids. The carbon atoms were refined isotropically; see the Experimental section for details.

Figure 7. Fast inversion of the bound ylide enantioface results in inversion of the chirality at the ylide carbon, as required for P-bound methyl and Cp^* group equivalency.

Figure 8. One possible mechanism of the fluxional process that results in equivalent PMe_2 groups and equivalent Cp^* rings, without intermolecular exchange.

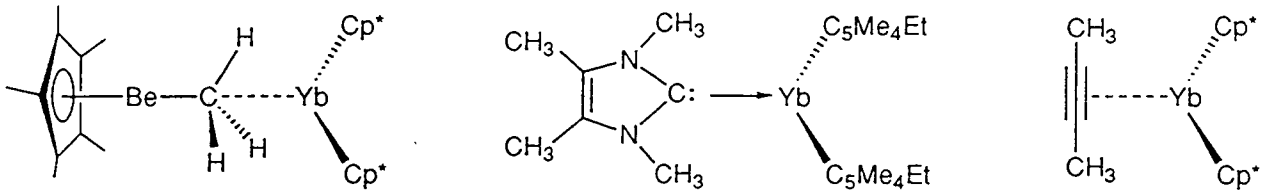
Be
C
H
H
H
Yb
Cp*
Cp*
CH3
CH3
N
C:
N
CH3
CH3
Yb
C5Me4Et
C5Me4Et
CH3
CH3
Yb
Cp*
Cp*

Figure 1.

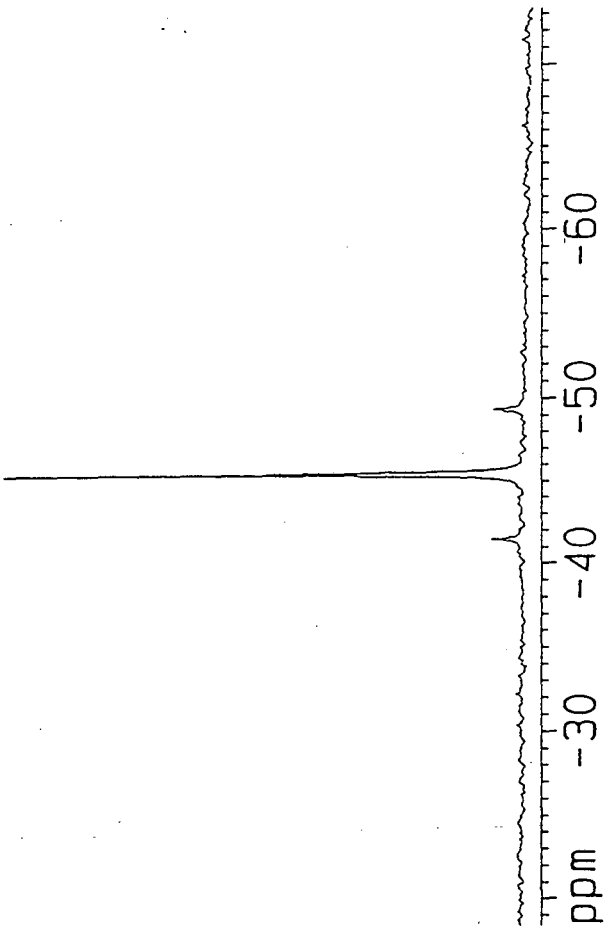

Figure 2

Figure 3

Figure 4.

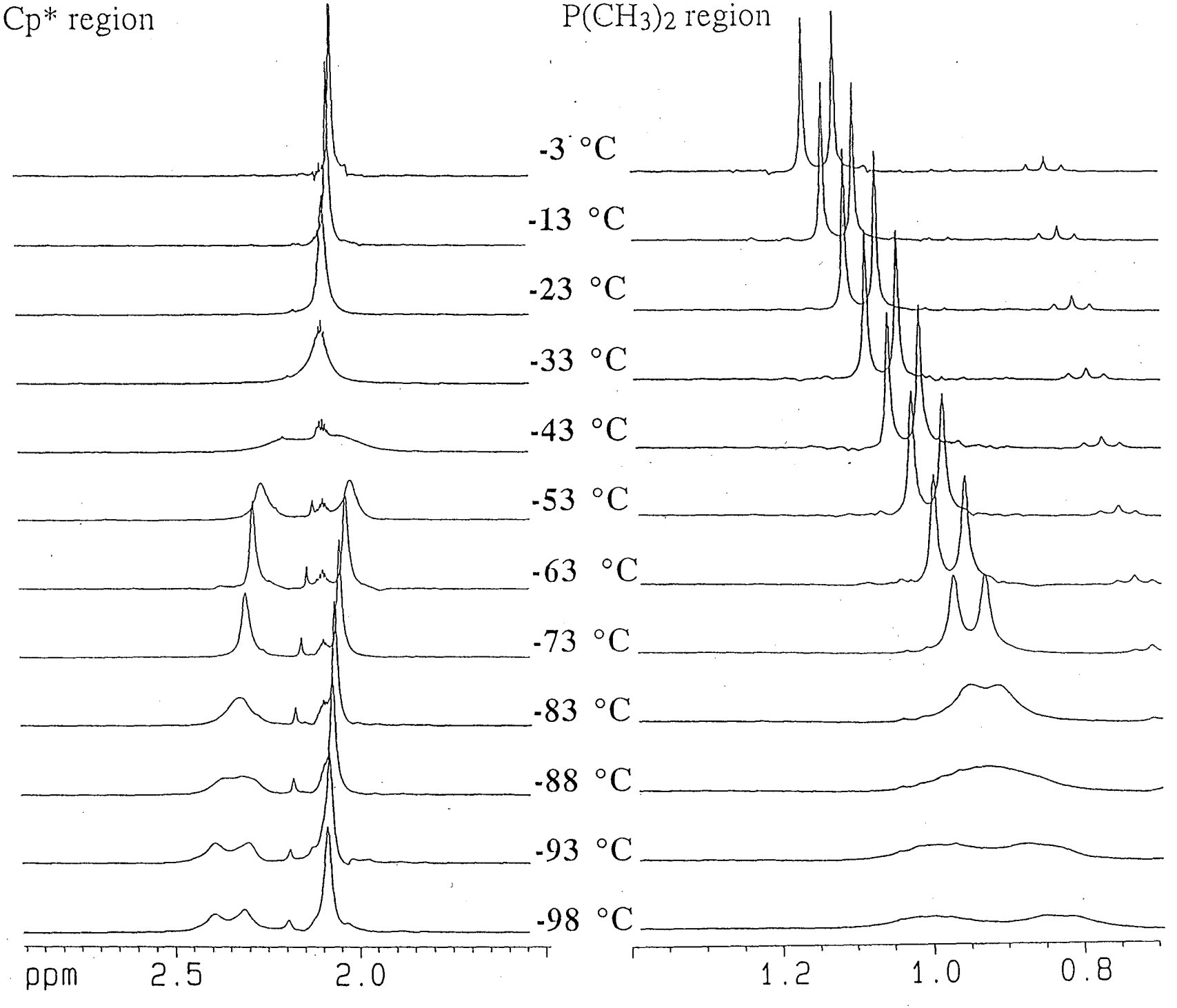
Cp* region
P(CH3)2 region
-3 °C
-13 °C
-23 °C
-33 °C
-43 °C
-53 °C
-63 °C
-73 °C
-83 °C
-88 °C
-93 °C
-98 °C
ppm
2.5
2.0
1.2
1.0
0.8

Figure 5

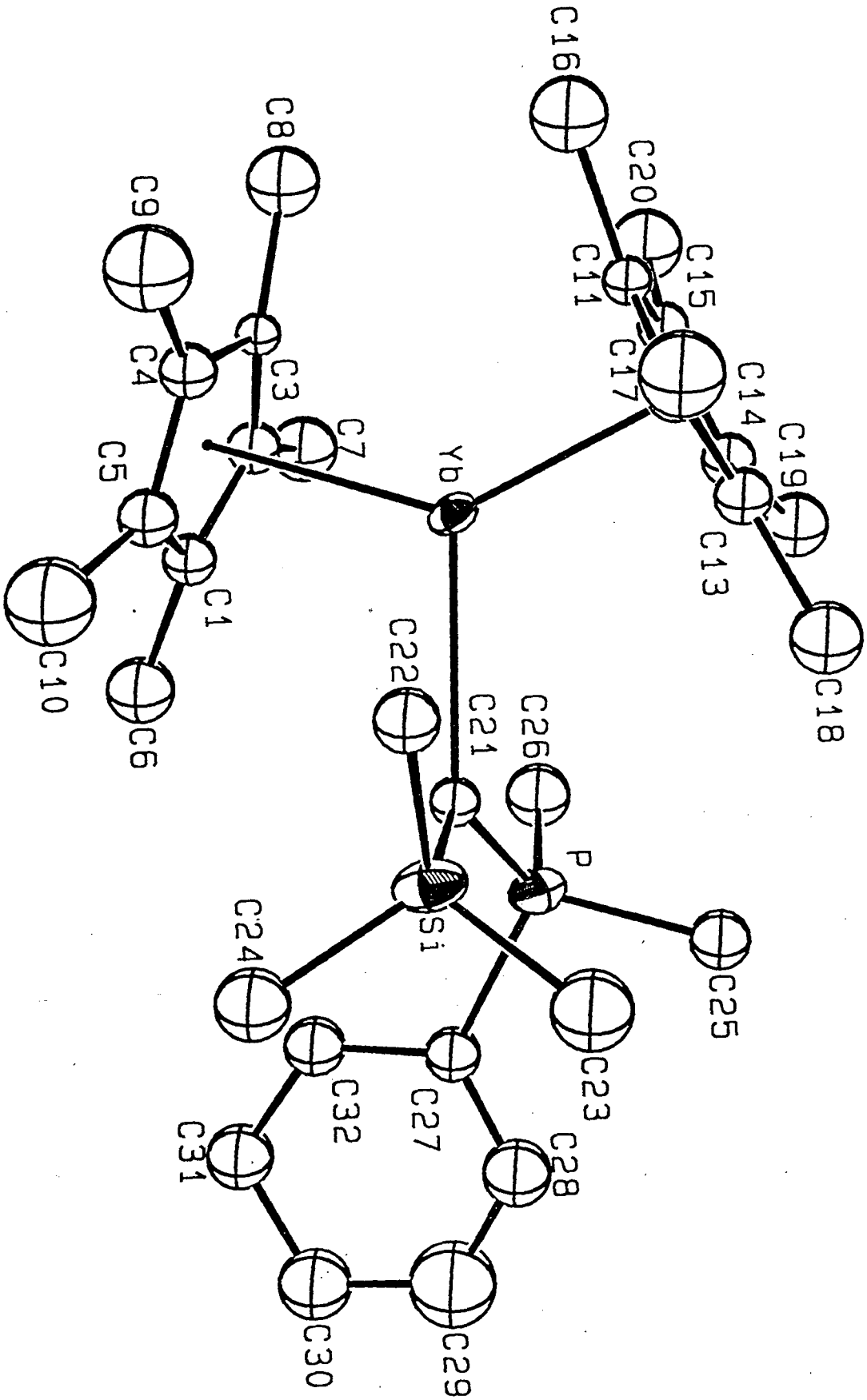
C16
C8
C20
C9
C15
C11
C4
C3
C17
C14
C7
C19
C5
Yb
C13
C1
C22
C18
C10
C21
C26
C6
P
Si
C24
C25
C23
C32
C27
C28
C31
C30
C29

Figure 6

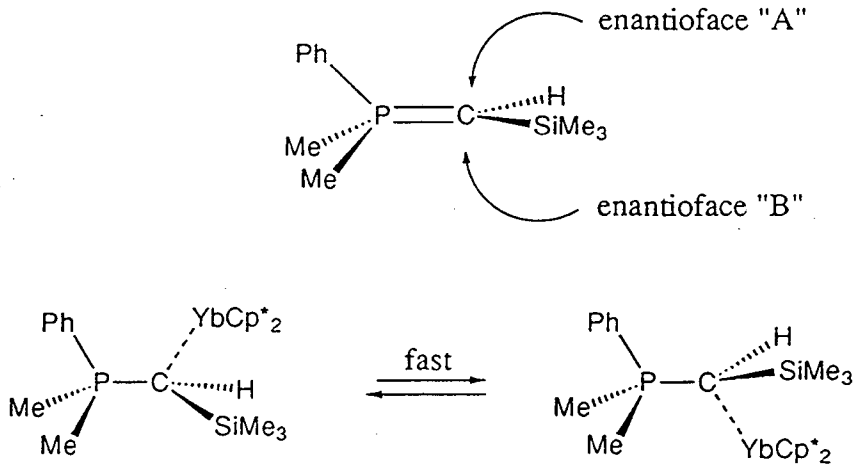
enantioface "A"
Ph
P
C
H
SiMe3
Me
Me
enantioface "B"
Ph
YbCp*2
P
C
H
Me
Me
SiMe3
fast
Ph
H
P
C
SiMe3
Me
Me
YbCp*2

Figure 7.

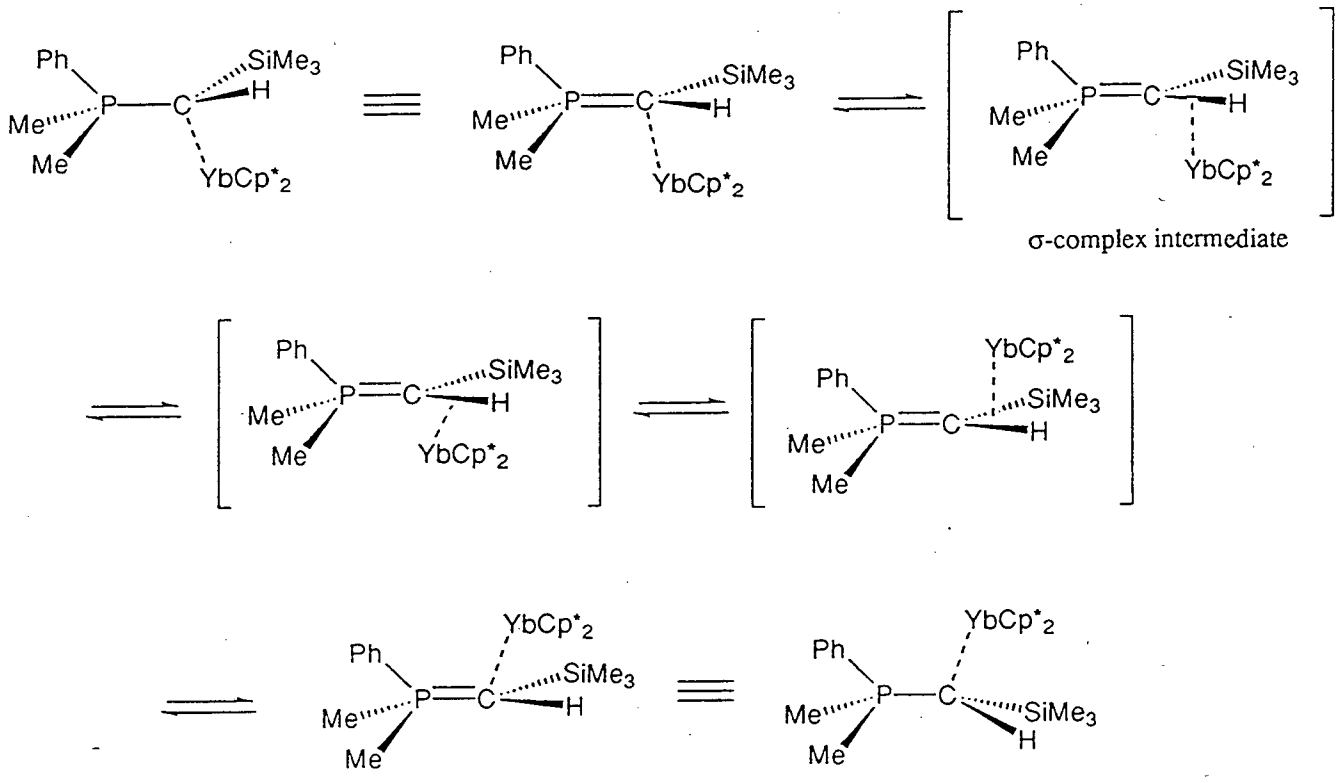

Figure 8.

LAWRENCE BERKELEY LABORATORY
UNIVERSITY OF CALIFORNIA
TECHNICAL INFORMATION DEPARTMENT
BERKELEY, CALIFORNIA 94720